

# Estimating forest carbon fluxes in a disturbed southeastern landscape: Integration of remote sensing, forest inventory, and biogeochemical modeling

Jeffrey G. Masek and G. James Collatz

Biospheric Sciences Branch, NASA Goddard Space Flight Center, Greenbelt, Maryland, USA

Received 8 June 2005; revised 20 September 2005; accepted 25 October 2005; published 2 February 2006.

[1] Quantifying carbon fluxes between the atmosphere and land surface requires detailed knowledge of the disturbance regime as well as the photosynthetic response of vegetation to climate. In this study, we use a combination of satellite remote sensing, forest inventory data, and biogeochemical modeling to assess forest carbon fluxes from central Virginia, a landscape pervasively disturbed by harvest. Using historical Landsat imagery, we have reconstructed the disturbance history and age structure of forest stands at a resolution of 90 m, from 1973–1999. Forest inventory data provide breakdowns of forest type and age structure for older stands. These data, together with climate and vegetation greenness from advanced very high resolution radiometer (AVHRR), are used as inputs to a version of the Carnegie-Stanford-Ames (CASA) biogeochemical model, which simulates the uptake, allocation, and respiration of carbon and associated effects of disturbance. Modeling results indicate that forests in the study region have an average net ecosystem productivity (NEP) of  $\sim 80 \text{ gC m}^{-2} \text{ yr}^{-1}$ , reflecting the young age structure of rapid-rotation forests. Variability in annual forest carbon fluxes due to variations in clearing rate and climate are also examined. We find that observed variations in clearing rate may account for NEP variability of  $\sim 30 \text{ gC m}^{-2} \text{ yr}^{-1}$ , while observed variations in climate may account for NEP variability of  $80\text{--}130 \text{ gC m}^{-2} \text{ yr}^{-1}$ . Increased temperatures tend to drive both increased photosynthesis and increased heterotrophic respiration, buffering the system from larger swings in NEP. However, this response depends strongly on stand age.

**Citation:** Masek, J. G., and G. J. Collatz (2006), Estimating forest carbon fluxes in a disturbed southeastern landscape: Integration of remote sensing, forest inventory, and biogeochemical modeling, *J. Geophys. Res.*, *111*, G01006, doi:10.1029/2005JG000062.

## 1. Introduction

[2] The consensus view is that about one quarter of the world's fossil fuel carbon emissions are being absorbed by land vegetation, through some uncertain combination of fertilization, climate enhancement of growth, and recovery from disturbance [e.g., Bousquet *et al.*, 2000; Battle *et al.*, 2000; Casperson *et al.*, 2000; Pacala *et al.*, 2001; Houghton *et al.*, 1999; Nemani *et al.*, 2002]. This conclusion reflects a long-term discrepancy between the observed increase of atmospheric carbon dioxide and known sources and sinks from fossil fuel emissions, tropical deforestation, and ocean solubility. However, this long-term perspective camouflages significant year-to-year variability. The annual rate of increase in atmospheric carbon dioxide has not been constant, but has varied from 1 to 5 Pg/yr since 1980 [Houghton, 2000] and is mainly driven by variability in the land sink [e.g., Battle *et al.*, 2000].

[3] Common process-based (“bottom-up”) approaches used to identify the nature of terrestrial carbon sources

and sinks include direct, local measurements using eddy flux methodologies [e.g., Barford *et al.*, 2001], analysis of forest inventory records [e.g., Turner *et al.*, 1995], and integration of historical land use records within biogeochemical models [e.g., McGuire *et al.*, 2001]. Each approach has limitations. While flux tower observations have been pivotal in linking physiologic processes to ecosystem carbon fluxes, the land area sampled by flux networks is too limited for regional and continental assessments [Saleska *et al.*, 2003; Thornton *et al.*, 2002]. These data may be used instead to calibrate biogeochemical models capable of simulating ecosystem fluxes forced by changing environmental conditions. Similarly, forest inventories can provide information on forest age and biomass, which can also be used to parameterize biogeochemical models. However, these inventories are often at decadal time steps and at spatial resolutions usually determined by political jurisdictions (such as counties in the case of the USFS Forest Inventory and Analysis or FIA Program).

[4] A variety of biogeochemical models have been published, generally using some combination of climate data, vegetation parameters, and remote sensing to estimate photosynthetic productivity of ecosystems. One common

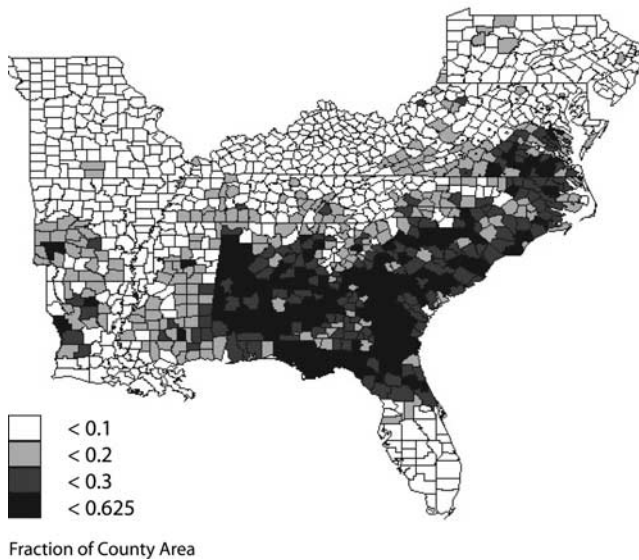


**Figure 1.** Map of southern and mid-Atlantic regions of United States, showing the percentage of each county occupied by young (<20 years old) timberland. The zone of rapid rotation pine forestry appears as a “belt” of young stands following the coastal and Piedmont physiographic zones of the region. Data are from U.S. Forest Service Forest Inventory and Analysis database.

difficulty has been the lack of information on regional disturbance patterns within forests. Disturbance events themselves (e.g. fire, insect defoliation, harvesting) tend to release large amounts of carbon to the atmosphere. Conversely, during recovery forests add biomass, sequestering carbon from the atmosphere. As a result, stand age, which depends directly on the disturbance history, is a strong determinant of net ecosystem productivity in forests. While some modeling studies have begun to incorporate disturbance [e.g., *Hurt et al.*, 2002; *McGuire et al.*, 2001; *van der Werf et al.*, 2004], most rely on coarse-resolution data sets that only resolve the largest events. Fully quantifying the effects of human-induced disturbances, including logging, harvest, land-cover change, and urbanization, requires regional data on disturbance history collected at high resolution. The 33-year Landsat record, used in this study, offers one useful source for this information [*Cohen et al.*, 2002].

[5] In this study we combine biogeochemical modeling, remote sensing, forest inventory, and eddy flux data to study forest net ecosystem productivity in central Virginia. The study region is representative of the southeastern United States, where rapid-rotation harvests of planted pine have led to a condition of “perpetual disturbance,” and the long-term replacement of natural pine and mixed-deciduous forest with young planted pine could have significant regional effects on carbon sources and sinks. Although the study area is relatively small, it offers a prototype for approaches that might be carried out on a continental scale. Our objectives are to (1) demonstrate a viable approach for incorporating both disturbance history and interannual climate variability within biogeochemical models in order to calculate realistic carbon fluxes; and (2) evaluate the relative

contributions of disturbance and climate to interannual variability of carbon fluxes from the region.

## 2. Southeastern Forests and Carbon Cycling

[6] The southeastern United States is composed of 13 states with a total forest cover of 86.9 million hectares (Mha) [*Conner and Hartsell*, 2002]. Approximately two thirds of timberland is comprised of hardwood dominated forests (oak-hickory, oak-pine, oak-gum cypress), and one third softwood types (loblolly and longleaf/slash pine). The total area of forested land in the southeast has declined by about only 5% since 1953, but this relative stability hides significant changes in forest management and ecology. Although the percentage of all pine forests has declined slightly since 1950, the area of planted pine has increased dramatically from near zero in 1950 to 12 Mha in 1999 [*Conner and Hartsell*, 2002]. Urban encroachment has also reduced forested areas within the last half century but this has been matched in part by abandonment and reforestation of previous agricultural lands. Reflecting decreases in clearing for agriculture since the early part of the twentieth century, the fraction of hardwood forests has increased from 46% in the 1950’s to 52% in 1999.

[7] Clearing and harvesting dominate short-term disturbance dynamics in the region. Wildfires do occur, but are always suppressed. In 1999 Virginia experienced a severe drought and worst fire season in 12 years yet the approximately 2500 Ha burned that year was small compared to about 81,000 Ha harvested each year in the state (<http://www.dof.virginia.gov/fire/va-fire-history.shtml>) Logging, therefore, is the major disturbance regime in this region. Management strategies range from traditional (only thinning) to high intensity (planting of productive hybrids, fertilization and weed control). The resulting landscape is a patch-work landscape, with a large component of young (<20 years old) forests representing the rapid-rotation pine plantations (Figure 1).

[8] The impact of harvest-regrowth cycles on the regional carbon balance is likely to be significant. *Turner et al.* [1995] used the ATLAS forest inventory projection model to predict mean annual carbon accumulation across the United States for the early 1990s, and concluded that the south-central and southeastern United States exhibited relatively high biologically driven NEP values ( $170 \text{ gC m}^{-2} \text{ yr}^{-1}$  and  $210 \text{ gC m}^{-2} \text{ yr}^{-1}$ , respectively). When integrated by area, these regions had the highest rates of carbon uptake in the nation ( $78 \text{ TgC/yr}$  and  $75 \text{ TgC/yr}$ , respectively).

[9] These rates reflect two phenomena. First, young forests tend to exhibit higher values of net ecosystem productivity due to the lag time between increasing net primary production (NPP) following disturbance and increasing heterotrophic respiration ( $R_h$ ) as biomass and detritus accumulates [e.g., *Odum*, 1969; *Litvak et al.*, 2003]. The spatial extent of young, recently harvested forests in the southeast contributes to the high regional NEP values. Second, the relatively long growing season, warm temperatures, and abundant precipitation result in relatively productive forests regardless of age [e.g., *Brown and Schroeder*, 1999]. It should be noted, however, that the productivity values given above only sum NPP and on-site

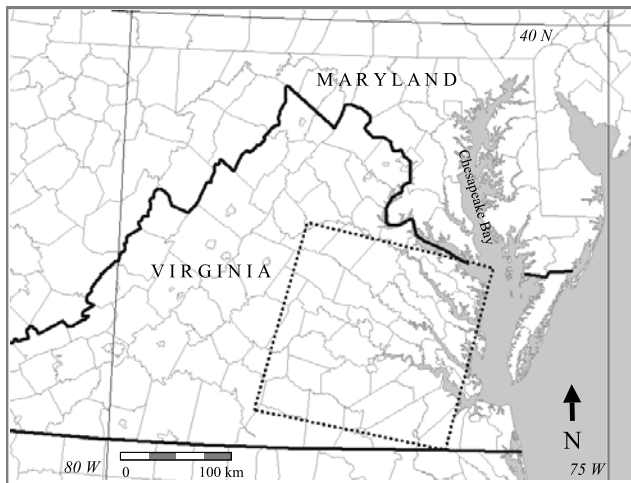


**Figure 2.** Central Virginia study area, showing the boundary of the Landsat image time series in dashed line.

emissions from soil and woody debris respiration. They do not include the emissions from the harvested products themselves. Including emissions from harvested wood and paper products may significantly lower (or eliminate) the net carbon sink arising from southeastern forests.

### 3. Analysis Methodology

[10] In this study we focus on central Virginia, which marks the northernmost area of rapid-rotation pine forestry in the southeast. The study area comprises one nominal Landsat TM scene (path 15 row 34), and extends from the coastal plains (dominated by lowland hardwoods and pines) to the Appalachian foothills (dominated by upland hardwoods) (Figure 2).

[11] The overall analysis framework used the historical Landsat record, forest inventory measurements, and biogeo-

chemical modeling to derive biomass and carbon flux estimates for the study region (Figure 3). Each of the modeling components is discussed below. We have two separate goals. First, we wish to create a spatially explicit map of mean net ecosystem productivity (NEP) for a reference year (1999) based on the regional disturbance history and mean climate conditions. Second, we wish to predict the relative roles of climate and disturbance in explaining year-to-year variability in carbon fluxes across the region. For clarity we note that our definition of NEP deviates from that of *Randerson et al.* [2002], in that we do not include transfers or emissions of harvested material, which are assumed to occur outside of the forest ecosystems considered here. Instead, the NEP values calculated here would reflect the impacts on the local atmospheric  $\text{CO}_2$  concentrations as would be measured by an aircraft sampling within the planetary boundary layer or by a flux tower situated within the forest environment itself.

#### 3.1. Regional Disturbance History

[12] The CASA biogeochemical model predicts net ecosystem productivity (NEP) via allocation of net primary production (NPP) to aboveground and belowground pools, which have turnover rates governed by specified rate constants. To a first approximation, stand NEP is strongly controlled by stand age, which is itself a function of the disturbance history. Our approach is to derive recent (<30 years) disturbance history from the analysis of Landsat satellite imagery (30-m resolution), while the age distribution of older forestland is derived from county-level Forest Inventory and Analysis (FIA) data. This approach relies on satellite data to obtain detailed disturbance dynamics for the last 3 decades (when NEP relations are expected to change most rapidly), but also permits inclusion of earlier dynamics using FIA stand age data.

[13] Recent disturbance and clearing can be mapped from an assembled Landsat image time series using spectral trajectories. Following disturbance, regrowing forests fol-

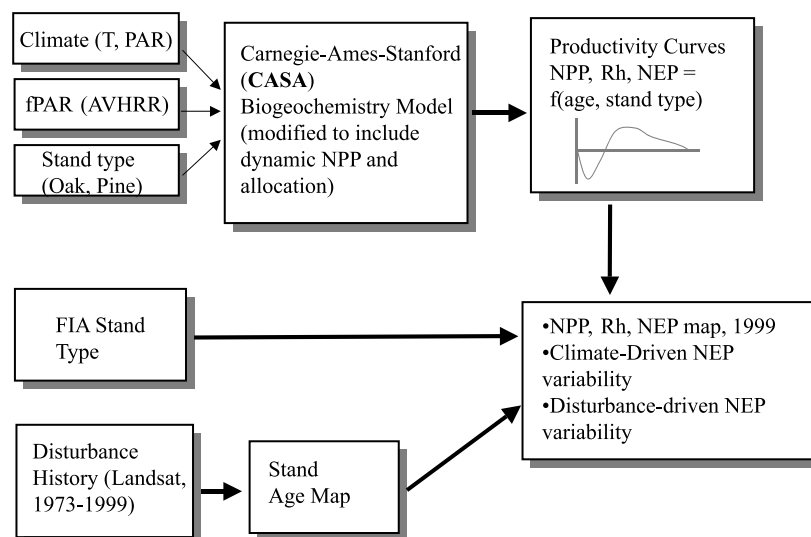


**Figure 3.** Schematic diagram showing the framework for the carbon flux analysis in this study. Long-term forest attribute information from the FIA and short-term disturbance information from Landsat analysis are integrated with CASA biogeochemical modeling to predict ecosystem fluxes.

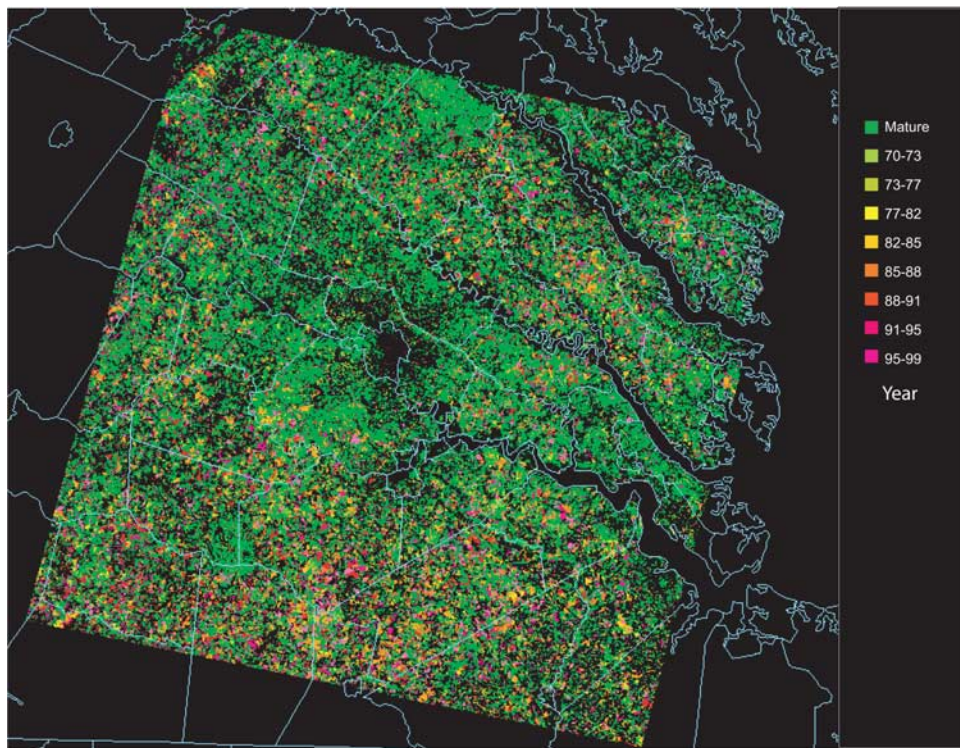


**Figure 4.** Map showing epoch of last disturbance for the Virginia study area. Black areas are nonforest regions including water, cropland, and urban areas.

low well-defined spectral paths, typically characterized by decreasing reflectance in the shortwave infrared and visible, and increasing values in the near-infrared. These changes, related primarily to structural changes within the canopy, tend to be consistent for any given stand type. Once these trajectories have been assembled, calculating the “time since disturbance” (essentially stand age for major disturbance) is simply a matter of stepping backward through the image time series, and marking the last spectral transition from “forest” to “cleared” [Cohen *et al.*, 2002].

[14] This technique was used here to calculate time since disturbance in central Virginia using a series of eight Landsat images acquired from 1973 to 1999. Most images were acquired during the early fall (15 September to 10 October), thus minimizing seasonal variations in image brightness. All images were coregistered, and radiometrically normalized using linear histogram matching to further reduce fluctuations in brightness. Digital numbers (DNs) were converted to surface reflectance by subtracting the darkest object in the image (“dark-object subtraction”), and then adjusting the calibrated at-sensor radiance for solar geometry, band-pass irradiance, and Sun-Earth distance. Clearing events were then identified on a per-pixel basis as described above, using fixed thresholds in the visible and short-wave infrared (for Landsat TM and ETM+) and the visible and near-infrared (for Landsat MSS).

[15] The resulting stand age map shows classes for each possible epoch of clearing since 1973 (Figure 4). The map illustrates the impact of rapid-rotation forestry on the age structure of Virginia’s forests, and also the significant

north-south gradient in the intensity of harvest. Forests in the northern part of the state share similar management regimes as other mid-Atlantic states (Maryland, Delaware, Pennsylvania), and are dominated by older hardwood or mixed hardwood stands. Forests in southern Virginia are more heavily disturbed, marking the transition to the planted pine regime.

[16] The accuracy of the disturbance map has been assessed in two ways. First, the “automated” (threshold-based) algorithm described above was compared to a visual analysis of the same Landsat imagery. A random group of 79 pixels was selected from the classified age map, and the disturbance history was interpreted visually using the ENVI image processing program. Overall agreement was found to be 80%. If the validation constraints were relaxed to permit the pixel to be within plus or minus one age class of that found through visual inspection, agreement increased to 89%. A second validation approach compared FIA stand-age distributions at the county-level with those found from the Landsat analysis. In particular, the area of very young forest in the FIA (<20 years old) should correspond to the area mapped as “cleared” during the last 20 years. In practice, since we don’t have an exact Landsat observation epoch from 1979–1999, the 20-year clearing area for each county was interpolated by taking the mean annual clearing rate since 1982 and multiplying by 20. The resulting values closely matched the areas of young forest from the FIA (Figure 5).

### 3.2. Forest Type

[17] To a first approximation, forests in Virginia are composed of young planted pine or relatively mature

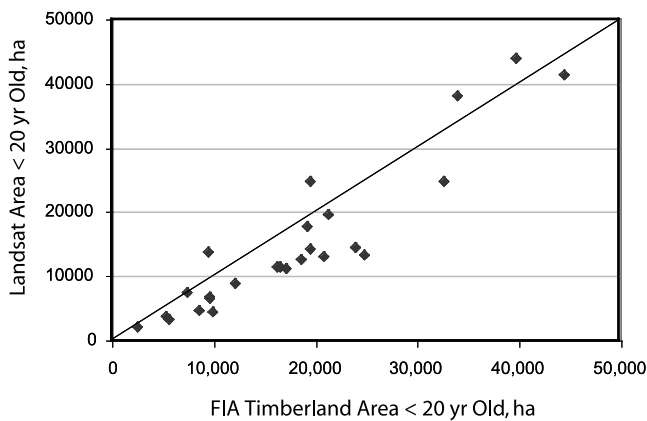


**Figure 5.** Relationship between the Landsat-derived area of young (<20 years old) forest and that from the U.S. Forest Service Forest Inventory and Analysis (FIA) database.

secondary hardwood (Figure 6). Young pure hardwood plantations are rare, as are older natural pine forests. Within the CASA modeling, we simplify ecosystem demography to include a generic planted pine (loblolly) and a generic hardwood (oak) type. We assume that forests undisturbed since 1970 are dominated by hardwoods. The age distribution of these older hardwood forests is derived from FIA statistics, and assigned a nominal age of 60 years old. We assume that younger forests disturbed since 1970 are dominated by planted pine, and the age of these forests is derived from the satellite data as described above.

### 3.3. Biogeochemical Model

[18] The modeling approach is based on the heterotrophic respiration component of the CASA biogeochemical model [Potter *et al.*, 1993]. In CASA NPP is calculated with a light use efficiency type model driven by satellite NDVI, PAR and scaled by temperature and moisture stresses (Figure 7). On a monthly time step NPP is allocated to leaves, roots and wood. Each of these pools has a turnover time that specifies the rate at which carbon moves to litter pools (surface fine litter, soil fine litter, coarse woody debris). The litter pools in turn decompose into slow and armored soil carbon pools at rates depending on up-stream pool sizes, temperature and soil moisture. The version of CASA used here incorporates responses to disturbance events (i.e., harvest) through the removal of carbon from biomass and litter pools, the redistribution of carbon left after disturbance to detritus pools and recovery of pools over time after disturbance. Specifics are as follows.

[19] 1. A disturbance event causes NPP to fall to a prescribed minimum level in the month of the disturbance and then recover over several years depending on specified parameters. The dynamics of recovery in NPP are parameterized to follow the recovery of FPAR/LAI after disturbance. After the forest has reached maturity NPP is scaled down from peak levels to mimic observed declines in NPP in mature forests [e.g., Gower *et al.*, 1997]. Allocation of NPP to wood is prescribed to increase with time after disturbance since initially most NPP is allocated to herbaceous growth with more going to wood as the stand ages [e.g., Law *et al.*, 2002; Jokela and Martin, 2000]. The

disturbance event causes the living biomass pools (leaves, roots, wood) to dramatically decrease (depending on the type and level of disturbance). Most of the root biomass is killed and transferred to soil carbon pools, and wood is removed. The fates of leaves, coarse woody debris and surface litter are determined by the type of disturbance (e.g., harvesting versus burning). Here a harvest event is prescribed as a 90% reduction in wood, leaf and surface litter pools and 80% mortality of the root pool.

[20] 2. After a disturbance event, carbon cycles through the system, toward establishment of a new equilibrium state at rates dependent on the turnover times of the pools and the meteorological conditions.

[21] A version of this dynamic recovery model has been used to estimate the carbon fluxes during recovery from fire in North American conifer forests [Hicke *et al.*, 2003].

### 3.4. Parameterization, Calibration, and Validation

[22] A number of model simulations were carried out using mean climate conditions in order to isolate the ecosystem response to harvest/regrowth cycles. Monthly precipitation, temperature and surface downwelling solar irradiance for the period 1989–1998 were obtained from the Global Precipitation Climatology Project (GPCP) version 2 precipitation data set ( $2.5^\circ \times 2.5^\circ$ , monthly, <http://precip.gsfc.nasa.gov> [Huffman *et al.*, 1997]), air temperature anomalies ( $2^\circ \times 2^\circ$ , monthly [Hansen *et al.*, 1999]) and the International Satellite Cloud Climatology Project Global Radiation Flux Data Products ( $2.5^\circ \times 2.5^\circ$ , monthly [Zhang *et al.*, 2004]) respectively. The mean monthly fraction of incident photosynthetic active solar irradiance absorbed by the canopy (fPAR) for the region was derived from the AVHRR normalized difference vegetation index (NDVI) product produced by the Global Measurement and Modeling System (GIMMS,  $1^\circ \times 1^\circ$ , monthly [Tucker *et al.*, 2006]). Where necessary, all input data sets were resampled and interpolated (bilinear) to  $1^\circ \times 1^\circ$ .

[23] We calibrated the dynamic recovery modeling using FIA growing stock volume data for selected counties in central Virginia that were dominantly either oak or pine forested. These data were used as inputs into a regression

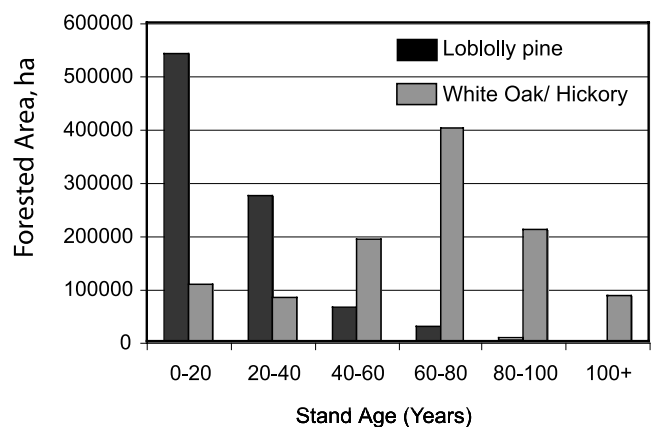


**Figure 6.** Forest area versus age distribution for pine and oak-hickory stand types, for all Virginia counties, from U.S. Forest Service Forest Inventory and Analysis (FIA) database.



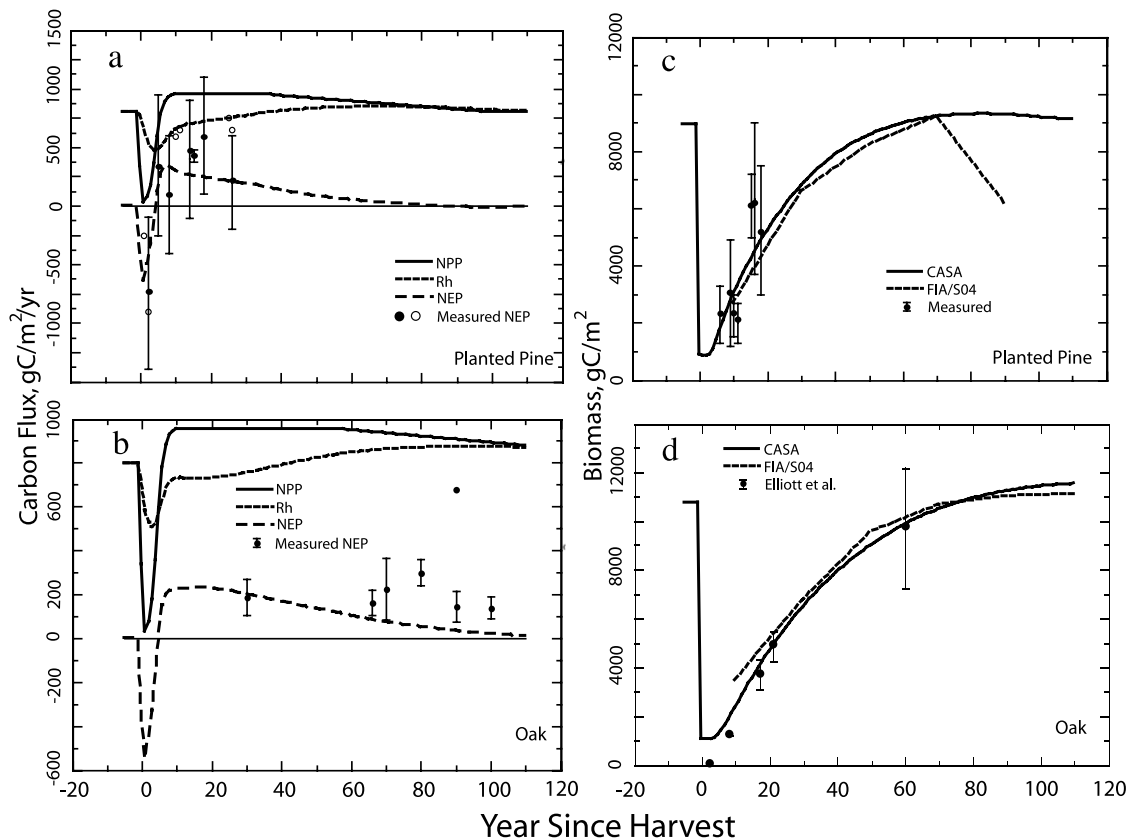


**Figure 8.** (a, b) Modeled carbon fluxes and (c, d) live biomass for pine and oak stand types, as function of time since stand-clearing disturbance. Model-derived curves for NPP (solid line), Rh (short-dashed line), NEP (dashed line), and biomass (solid line) are shown. Simulations used mean climatology for central Virginia study area. The CASA model was initialized by running for 1500 years before Year 0, in order to stabilize belowground soil pools before the disturbance event. Note that ecosystem carbon fluxes do not include emissions from harvested material exported from the site. Superposed on the model-derived curves are observational data from field biometry, and flux studies (means and ranges [Janssens *et al.*, 2001; Curtis *et al.*, 2002; Barford *et al.*, 2001, Elliott *et al.*, 2002]). Superposed on the modeled biomass curves are biomass trajectories derived from FIA timber volume data converted to biomass using the relations of Smith *et al.* [2003].

average annual fluxes, although the disturbance history is particular to the date of the last image (September 1999). The resulting maps of NPP, Rh, and NEP indicate significant local heterogeneity as a result of harvest (Figure 9). The southern part of the study area, where harvest has been most intense, shows isolated patches of low NPP corresponding to very young planted pine clearings. However, planted pine NPP values rise rapidly, and within 10 years reach a maximum value. In contrast, heterotrophic respiration levels remain more constant during the disturbance cycle, dropping following disturbance, and rising slowly as biomass accumulates (and turns over) within the stand.

[28] The mean NEP across the forested part of the study region is calculated as  $84 \text{ gC m}^{-2} \text{ yr}^{-1}$ , positive values indicating net fluxes from the atmosphere to the land. This value is roughly equivalent to that of a mature (60–80 years old) oak stand ( $\sim 80 \text{ gC m}^{-2} \text{ yr}^{-1}$ ). To a first approximation, net carbon emissions from recent clearings nearly balance the carbon sink from regrowing stands. However, this balance hides significant spatial variability. For example,

roughly 15% of the forest area exhibits high NEP values in excess of  $200 \text{ gC m}^{-2} \text{ yr}^{-1}$  (net sink), while roughly 10% of the forest area exhibits values less than  $-200 \text{ gC m}^{-2} \text{ yr}^{-1}$  (net emission).

#### 4.2. Climate-Driven Variability in Carbon Fluxes

[29] One objective of this study was to quantify the relative contributions of climate-driven and disturbance-driven variability in ecosystem carbon fluxes. The productivity of vegetation systems respond to regional variations in temperature, precipitation, length of growing season, and available solar radiation. In CASA, anomalies in temperature and soil moisture are treated as scalars such that

$$\text{NPP} = \epsilon(T, \theta) \times \text{FPAR} \times \text{PAR}, \quad (1)$$

where  $\epsilon(T, \theta)$  represents the scalar light use efficiency integrating the effects of temperature and soil moisture, fPAR is derived from monthly AVHRR NDVI values [Los *et al.*, 2000], and PAR is derived from the monthly

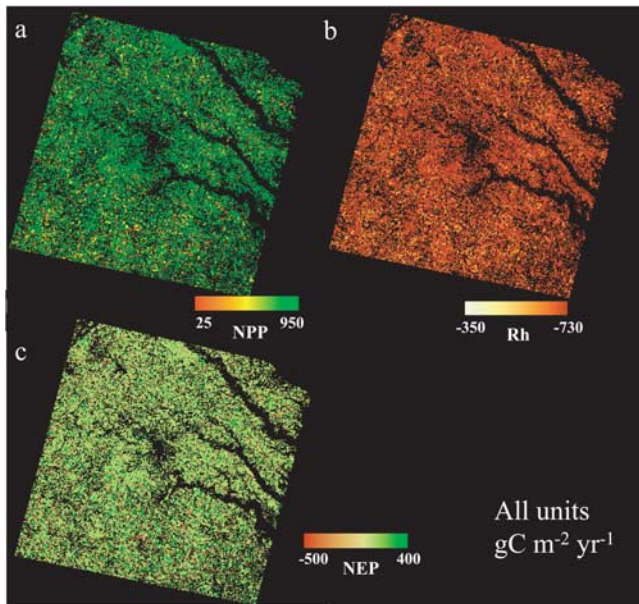


**Figure 9.** Maps of calculated mean annual (a) net primary production (NPP); (b) heterotrophic respiration (Rh); and (c) net ecosystem production (NEP), using the CASA model. Values use the stand age distributions derived for the year 1999, but mean climate conditions as in Figure 8.

climatologies At the same time, heterotrophic respiration of detritus carbon depends on soil temperature and soil moisture, modeled in CASA according to a “Q10” dependence. Thus climate variability primarily affects primary production and heterotrophic respiration independently though there is a slight dependence of heterotrophic respiration on past NPP.

[30] To examine the net effect of climate and fPAR variability on annual carbon fluxes, we examined the monthly temperature, precipitation and fPAR for the period 1982–2000 for the central Virginia region, and selected a recent 10-year span (1989–1998) that included significant excursions in both climate and fPAR (Figure 10). An alternate approach would have been to look at all possible combinations of temperature, precipitation, and radiation anomalies, and perform simulations for each combination. However, it is clear from the climate records that these variables tend to covary, and therefore independent combinations of anomalies do not occur physically. Thus using the variability from actual climate records gives a more plausible scenario for quantifying carbon variability.

[31] CASA has the capability to simulate soil moisture feedbacks on productivity using a “bucket” model. However, simulations that included precipitation variability indicated that modeled productivity in Virginia forests was not limited by water availability even during the low rainfall year of 1995 (the driest year for the period 1982–2003), so precipitation was eliminated as a driving variable from the CASA simulations. While the lack of sensitivity to precipitation may be in error, previous studies of regrowing young pine plantations given supplemental irrigation treatments also show that SE pine forests are not strongly water limited [Jokela *et al.*, 2004; Albaugh *et al.*, 2004].

[32] Forest responses to the 10-year climate (temperature, solar radiation) and fPAR records were simulated for three different stand-age cohorts for both pine and oak forest types: “young” (0–10 years), “medium aged” (30–40 years), and “old” (100+ years) stands. These classes allowed us to investigate how climate variability influences carbon fluxes across a range of stand ages and types. The model was first initialized with the mean monthly climatology for the 10-year period and run for 1500 years in order to stabilize soil carbon pools. Simulations for each age cohort were performed independently. The disturbance event (harvest) was then imposed and the climate for 1989–1998 was used to force the model in each of the disturbance age scenarios.

[33] The modeling results, presented as annual net C flux anomalies, indicate peak-to-peak climate-driven NEP variability of 80–130  $\text{gC m}^{-2} \text{yr}^{-1}$  (Figure 11). The range depends on the stand type and age cohort. In general, NPP and Rh tend to covary: Warmer conditions that lead to higher rates of primary production also lead to higher rates of heterotrophic respiration. The relationship between can be compared to that derived from long-term eddy-flux measurements at Harvard Forest [Barford *et al.*, 2001]. These observations indicate a consistent correlation between the magnitude gross primary production (GPP) and ecosystem respiration, noting that autotrophic respiration is implicitly accounted in CASA via NPP while ecosystem respiration measured at Harvard Forest includes both autotrophic and heterotrophic components (Figure 12). As a result of covariance between productivity and respiration, the variability of NEP is less than the variability of the component fluxes. In essence, the carbon fluxes from these forested ecosystems appear to be “buffered” with respect to climate variability. For CASA, variability in NPP also tends to be larger than that of Rh, so that the overall annual variability in NEP tends to follow the NPP anomaly.

[34] It should be noted that some exceptions to these patterns do occur. For example, in 1996 and 1997, high rates of NPP were driven by high fPAR values rather than climate. As a result, there was no correlation between NPP and Rh anomalies, and relatively low temperatures caused decreased heterotrophic respiration. Although the magnitudes of the individual anomalies were small, the fact that they were anticorrelated led to relatively large positive NEP anomalies (sink) during those years.

[35] Forest type appears to make relatively little difference with respect to interannual carbon flux variability. Pine and oak stands of the same age respond similarly to the 10-year climate record, and the overall magnitude of variability is only slightly higher for the oak case. However, stand age in either type makes a significant difference. Young stands exhibit the least NEP variability (80–90  $\text{gC m}^{-2} \text{yr}^{-1}$ ), while middle-aged stands exhibit the greatest (120–130  $\text{gC m}^{-2} \text{yr}^{-1}$ ). This behavior reflects the fact that NEP variability is dominated by variability in NPP, and the variability in NPP tends to follow its absolute value. Young stands, with low levels of NPP, tend to have reduced levels of NEP variability. Conversely, middle-aged stands, with the highest rates of NPP, demonstrate higher levels of NEP variability. The average NEP variability across the central Virginia

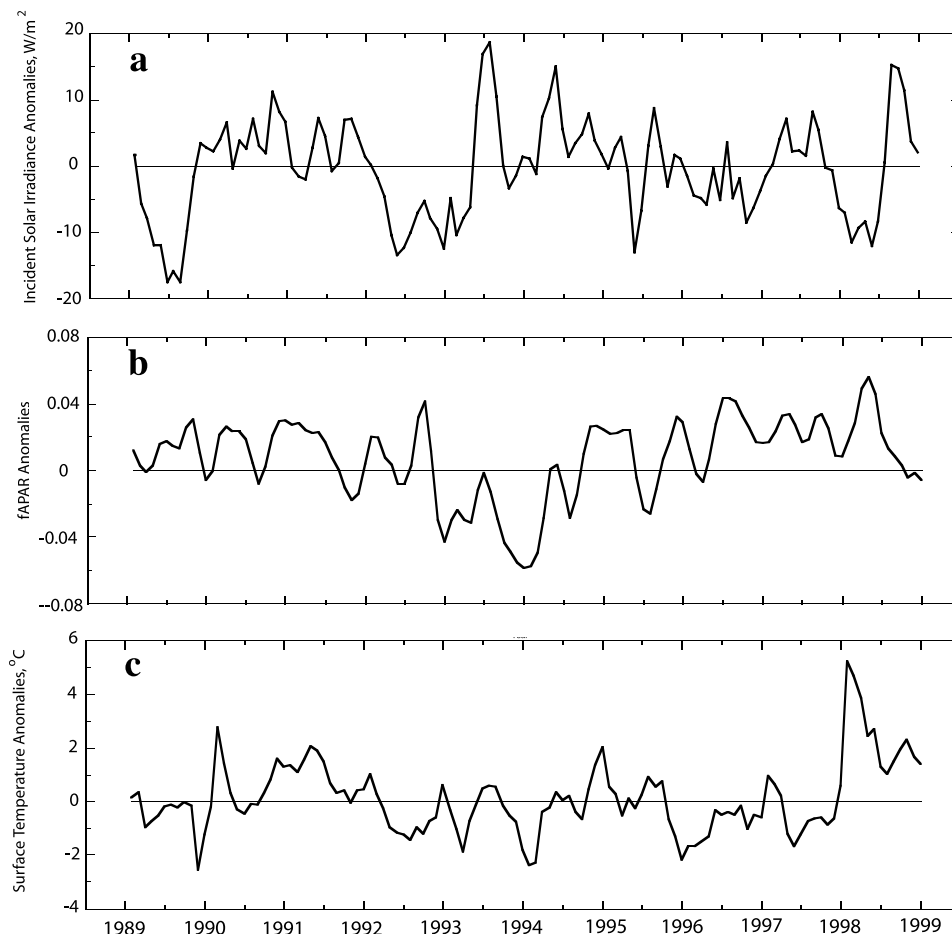


**Figure 10.** Incident solar radiation, fPAR, and temperature anomalies for Virginia, 1989–1998, used to calculate NEP response to climate/fPAR variability. Data are from *Huffman et al.* [1997], *Hansen et al.* [1999], and *Zhang et al.* [2004].

study area can be obtained by weighting the NEP variability of each forest type and age cohort by their relative areas. Using the data from the FIA (Figure 6), we calculate a regional interannual variability (peak-to-peak) of  $110 \text{ gC m}^{-2} \text{ yr}^{-1}$ .

[36] It is also worth comparing the relative contributions of climate variables (temperature, radiation) to fPAR in controlling NEP variations. The model was run holding either the climate driver or fPAR constant, and allowing the other driver to vary according to the 10-year record shown in Figure 10. The results indicate that each driver makes a roughly equal contribution to overall NEP variability (Figures 13a and 13b). As noted above, while the climate drivers control both NPP and Rh, variations in fPAR only affect NPP. NPP is affected by both solar irradiance and temperature (climate) while Rh is sensitive to temperature alone. The relative sensitivities of NPP and Rh to temperature depends on the season. At the peak of the growing season NPP is less sensitive to temperature than Rh while the reverse is true outside the growing season (not shown). Small variations in Rh in Figure 13b reflect the minor role played by allocation of short-term productivity gains to rapid turnover leaf, litter, and soil pools. The results illustrate this characteristic of CASA:

that NPP and Rh co-vary because of a common response to climate drivers, not through changes in allocation driven by NPP.

#### 4.3. Disturbance-Driven Variability in Carbon Fluxes

[37] Rates of forest harvest vary from year to year as individual growers respond to variations in demand and pricing. There is also good evidence for progressively more intensive harvest practices (i.e., shorter rotation periods) during the last 30 years [*Birdsey and Heath, 1995; Conner and Hartsell, 2002; Prisley and Malmquist, 2002*]. During this time, commercial forests in the southeast have become intensively managed through thinning and fertilization, forest productivity has risen, and rotation periods have shortened. These variations in clearing lead to long-lasting perturbations in the forest age structure, which in turn affect ecosystem carbon fluxes.

[38] Interannual changes in clearing are not well quantified from decadal forest inventories, but can be readily extracted from the Landsat-derived disturbance history. The image time series shows a mean clearing rate of 29,000 ha/yr (1.7% of forest area per year) since 1985, with a range of 23,000 to 36,000 ha/yr (1.3–2.1% forest area per year). Whether these are short-lived “spikes” in

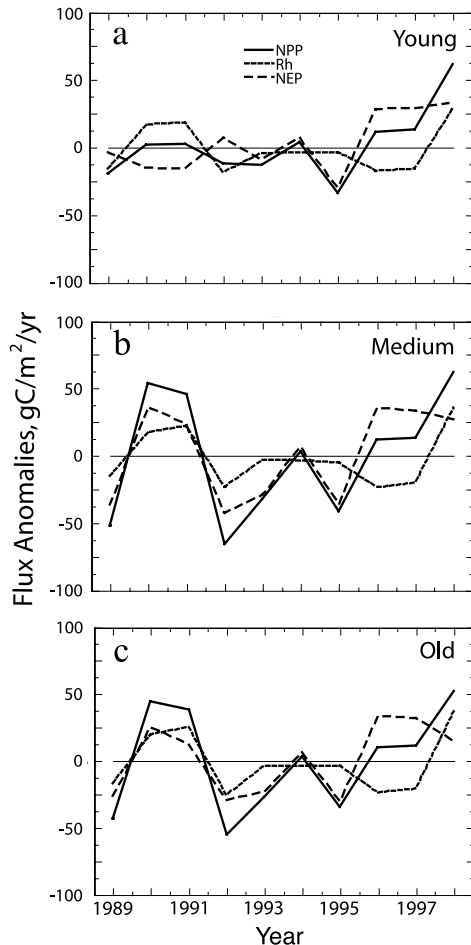


**Figure 11.** Effect of climate and fPAR variability on carbon fluxes. Plots show NPP, Rh, and NEP anomalies (deviations from mean climatology case in Figure 8) for pine, using 10-year climatology from Figure 10, for three different stand age cohorts: (a) young (<10 years), (b) medium aged (30–40 years), and (c) old (>100 years).

individual years, or more persistent trends over 3–5 years cannot be determined from the current data set.

[39] To model the effects of disturbance variability on ecosystem carbon fluxes, we use a simple inventory model

coupled to the CASA-derived NEP curves discussed above. As before, we assume two populations of forest stands: oak in long-term secondary growth and short-rotation planted pine. The age distribution of oak is held constant using a Gaussian distribution with a mean of 60 years, and a standard deviation of 30 years, analogous to the distribution shown in Figure 6. Initially pines are given an even age distribution from 0 to 80 years. We then prescribe a pine clearing history (fractional area of pine cleared each year). The age distribution of pine is incremented by 1 year each time step, and the amount of clearing for that year is extracted from cohorts aged 25–30 years (corresponding to the typical rotation period). This fractional cleared area is returned to the youngest (age zero) cohort, simulating the initiation of regrowth on cleared stands. We also assume that 10% of pines aged 40–80 are removed each year through clearing or mortality. Any remaining pines in the 80-year old cohort are assumed to die. These removals are also added to the zero-age cohort.

[40] Given the age distribution for any given year, we calculate the total landscape carbon flux as the product of the age histogram and the appropriate CASA-derived NEP curve for that stand type,

$$C_f(t) = \sum A_o(i) * N_o(i) + \sum A_p(i) * N_p(i), \quad (2)$$

where  $C_f(t)$  is the total annual forest carbon flux as a function of simulation year  $t$ ,  $A_o(i)$  and  $A_p(i)$  are the distributions of oak and pine area by age cohort  $i$ , and  $N_o(i)$  and  $N_p(i)$  are the annual oak and pine NEP fluxes for age cohort  $i$ . The NEP values  $N_o(i)$  and  $N_p(i)$  are calculated from the distributions shown in Figure 8, which were run using the mean regional climatology. Unlike the simulations presented in section 4.2, effects of interannual variations in climate and fPAR are not included. While very simple, the model does allow a first-order examination of how variations in clearing rate propagate to affect ecosystem-level carbon fluxes.

[41] Results from two different clearing histories are presented in Figures 14 and 15: a periodic “sine” wave variation in clearing rate (period = 40 years), and a random “white noise” variation. In both cases clearing rates varied from 1.5% to 2.5% per year, similar to the variability

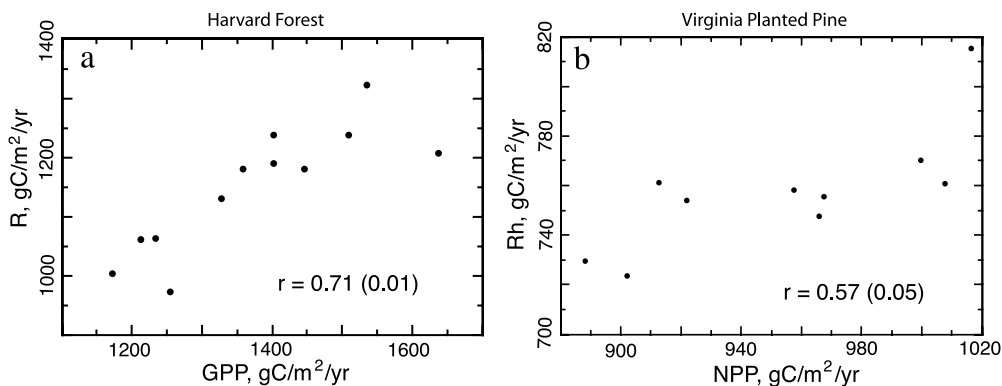


**Figure 12.** Relationship between photosynthetic productivity (GPP or NPP) and respiration (total or heterotrophic), for (a) Harvard Forest, from eddy-correlation flux tower data, and (b) Virginia planted pine, from CASA modeling.

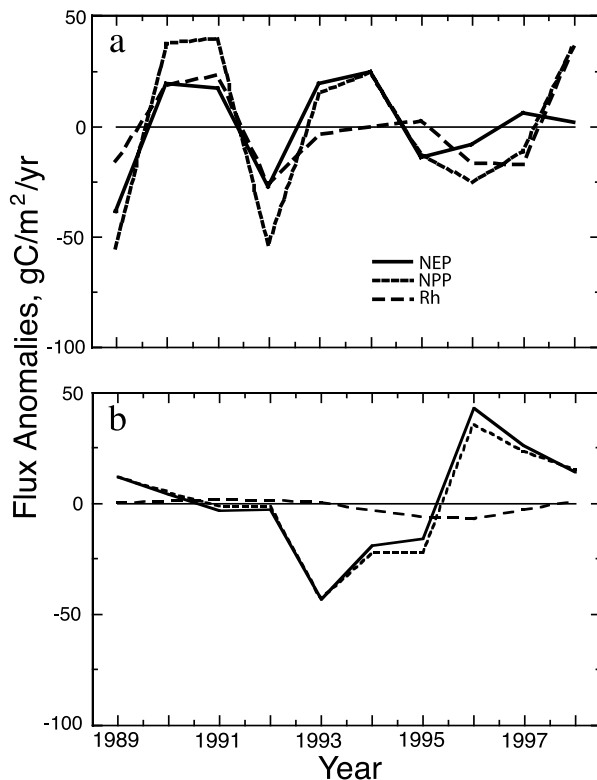


**Figure 13.** Modeled carbon flux variability due to (a) only variations in climate parameters (temperature, PAR) with fPAR held constant, and (b) only variations in fPAR with climate held constant. Note that climate variability drives most of the variability in both Rh and NPP, while fPAR only drives most of the variability in NPP.

derived from the image time series for central Virginia. The simulations were run for 300 years. Since 50–100 years of simulation were required to converge on a stable stand age distribution, only results from years 100 through 300 are presented here.

[42] Because NEP as a function of stand age changes relatively slowly, the system acts like a low-pass filter. Rapid (annual) fluctuations in clearing rate have a less pronounced effect on aggregate NEP than do fluctuations that persist over several years. Thus the “sine” wave clearing history, simulating long-lasting variations in clearing rate, results in peak-to-peak NEP variability of  $69 \text{ gC m}^{-2} \text{ yr}^{-1}$  while the rapidly fluctuating “white noise” history results in peak-to-peak NEP variability of just  $33 \text{ gC m}^{-2} \text{ yr}^{-1}$  (Figures 14 and 15). Persistence in clearing rate can arise from economic factors (price of wood and paper products) or through land-management policies at the county, state, or national level. An analysis of the clearing history in the Pacific Northwest using Landsat imagery revealed systematic variations in clearing rate related to forest management strategy over the last 30 years [Cohen *et al.*, 2002]. Similar results have been found for tropical deforestation rates in the Amazon where clearing rates declined during the early 1990s [Houghton, 2000]. From the satellite record of clearing in central Virginia, it appears that clearing rates can fluctuate on timescales of 3–5 years,

suggesting that the “white noise” model may be more appropriate.

## 5. Discussion

### 5.1. Regional Ecosystem Productivity

[43] We find that forests in central Virginia act as a biologic carbon sink, with an average biologic NEP of  $\sim 80 \text{ gC m}^{-2} \text{ yr}^{-1}$ , reflecting the balance between high emissions from recent clear cuts and high uptake by young regrowth. This figure refers simply to the net ecosystem productivity of the forest cover itself: Emissions from harvested wood and paper products are not included, and would act to depress the NEP value. This average NEP is significantly lower than the  $\sim 210 \text{ gC m}^{-2} \text{ yr}^{-1}$  found by Turner *et al.* [1995] for the entire southeast United States, probably reflecting regional conditions in Virginia as well as high rates of soil respiration following disturbance, which were not modeled by Turner *et al.* [1995]. The CASA simulations also assumed that the initial harvest event cleared primary (>200 year old) forest. Hence the initial soil carbon pools and their respiration fluxes were large. Assuming that the land had been in an agricultural condition prior to pine forestry would have led to smaller soil carbon pools, reduced soil respiration, and higher overall NEP values during the simulations. Assuming that most of the harvested land consisted of planted pine, with a harvest age of 25 years, we calculate a harvest removal of  $\sim 2.4 \text{ TgC}$  per year using the CASA wood and leaf pools.

[44] Comparisons of CASA results with observed fluxes and biomass data reveal large uncertainties, reflecting the limited constraints provided by current observations. In general, our simulations show a weaker carbon sink for recovering forests compared to eddy covariance studies. Our approach calibrated CASA to fit the FIA-based biomass

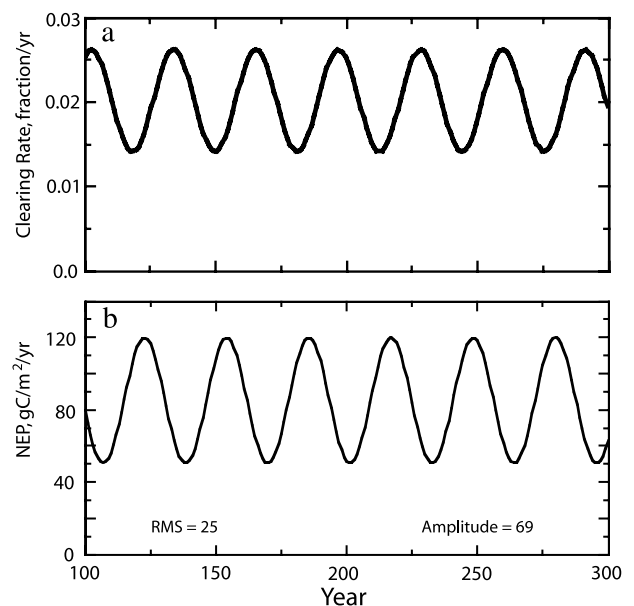


**Figure 14.** Simulated interannual variability in NEP arising from disturbance. (a) Simulated “sine wave” clearing history. (b) Calculated NEP history derived from the clearing history in Figure 14a.

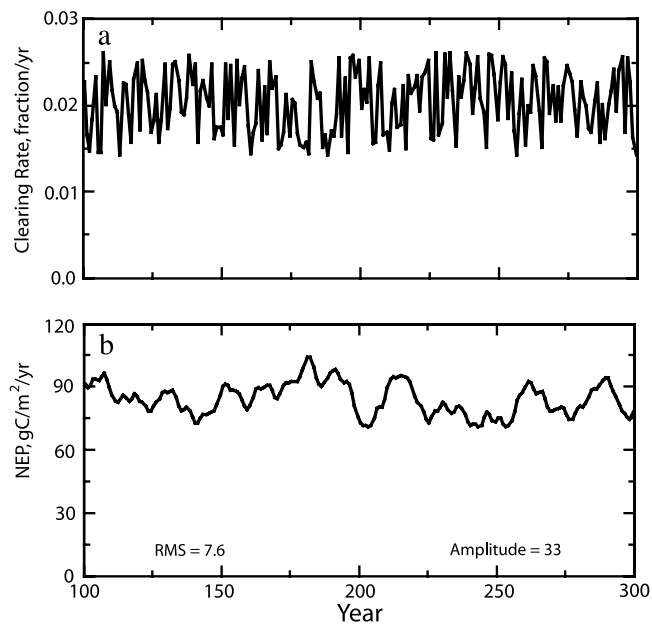


**Figure 15.** Simulated interannual variability in NEP arising from disturbance. (a) Simulated “white noise” clearing history. (b) Calculated NEP history derived from the clearing history.

estimates for the region, taking advantage of the large FIA database that is available, and which could be extended nationwide. The decreasing slope of the FIA-derived age-biomass accumulation curve requires that the modeled sink flux decrease in parallel. For pine, given the large uncertainties and landscape-scale variability in NEP and biomass, our simulated dynamic responses seem plausible, though perhaps at the lower end of the range of reported productivity. This is not surprising given that in Virginia around 80% planted pine forestry occurs on non-industrial private lands which tend to be made up of small tracts where intense management is more difficult and expensive [Siry, 2002]. In contrast, eddy correlation measurements tend to indicate higher fluxes for older forests than indicated by FIA biomass data (Figures 8a and 8b).

[45] It is clear that detailed knowledge of forest age structure is essential for predicting regional NEP. Numerous studies have pointed out that ecosystem productivity reaches a peak for young and middle-aged forests, as increasing soil/litter respiration and mortality lags behind increasing NPP [Odum, 1969; Turner *et al.*, 1995; Thornton *et al.*, 2002; Litvak *et al.*, 2003]. In the case of Virginia, the constant turnover of loblolly stands yields a mixture of very young (carbon source) and slightly older (carbon sink) stands, resulting in a near balance of NEP. Superposed on this “cropping” pattern is the steady aging of secondary hardwood and mixed hardwood/conifer forests. Much of the hardwood forest land regenerated during the 1930s to 1950s following the enactment of conservation policies and abandonment of agricultural lands [Conner and Hartsell, 2002]. These forests now act as a moderate, but persistent carbon sink.

[46] The carbon cycle model employed here does not explicitly simulate nutrient cycling. It would be expected

that harvest leads to the removal of nutrients such as nitrogen from the site and could exacerbate nutrient limitations on both productivity and decomposition. In fact, studies of the impacts of harvest on nutrient dynamics in mixed forests and pine forests in the southeast often show relatively small changes in soil nitrogen [Knoepp and Swank, 1997; Swank *et al.*, 2001; Johnson and Curtis, 2001]. Recovery after harvest will depend on management practices and soil type. While pine plantations in the southeastern United States respond strongly to nitrogen fertilization [Jokela *et al.*, 2004], fertilization tends to be employed by the commercial forest industry on large tracts. Fertilization is not economically viable on smaller, private (nonindustrial) tracts characteristic of the region considered in this study. Given the paucity of information that could be used to parameterize and test a more complex model that explicitly includes nutrient cycling, we have elected to use the simpler approach in this study. In addition, our calibration to regional FIA biomass data implicitly includes the impacts of nitrogen cycle responses to harvest. We recognize, however, that soil condition is likely to have strong controls over recovery dynamics and its inclusion in future work would represent an important improvement to our modeling framework.

[47] How will carbon fluxes evolve in the future? The current trend in the southeast is toward increasing areas of planted pine, decreased rotation rates, and increased intensity of management. There is some evidence that the more efficient management (fertilization, site preparation, thinning), possibly coupled with climate change, has resulted in increased rates of NPP in this region over the last 20 years [Hicke *et al.*, 2002]. However, decreased rotation rates, and the natural aging of secondary hardwood forests, will tend to decrease the area of middle-aged forests, and thus reduce the biologic carbon sink in coming decades.

## 5.2. Interannual NEP Variability

[48] The CASA simulations predict that forests in Central Virginia exhibit  $\sim 80\text{--}130\text{ gC m}^{-2}\text{ yr}^{-1}$  of peak-to-peak NEP variability due to climate and fPAR drivers, and about  $\sim 30\text{ gC m}^{-2}\text{ yr}^{-1}$  due to variability in disturbance rates. Assuming that these factors are independent of each other, climate variability accounts for 75% of NEP variability, with disturbance accounting for the remaining 25%. These results suggest that cold years, with low PAR and fPAR conditions, could cut the sink strength by  $40\text{--}60\text{ gC m}^{-2}\text{ yr}^{-1}$  (roughly 50–75%). Combining these conditions with high rates of harvest could reduce the sink strength another  $\sim 15\text{ gC m}^{-2}\text{ yr}^{-1}$ . Thus, under rare conditions, the annual biologic carbon sink in this region of  $\sim 80\text{ gC m}^{-2}\text{ yr}^{-1}$  could be nearly neutralized.

[49] A number of papers have documented how gross photosynthetic productivity varies as a function of precipitation and biome [Le Houerou *et al.*, 1988; Richard and Pocard, 1998; Knapp and Smith, 2001]. In general, forested biomes exhibit less response to precipitation variability than grasslands or semi-arid environments. However, it is important to consider the full range of climate parameters when examining susceptibility of ecosystems to climate variability. Like central Virginia many forested ecosystems are not water limited, and it is

**Table 1.** Interannual Variability in NEP Values

	Age	Mean NEP	NEP Standard Deviation	NEP CoV
CASA pine	30–40	194	31	0.16
	100+	–14	26	1.8
CASA oak	30–40	180	29	0.16
	100+	25	23	0.93
Harvard Forest	65 <sup>a</sup>	200	36	0.18

<sup>a</sup>Seventy percent of crown area removed by 1938 hurricane and salvage [Barford *et al.*, 2001].

unlikely that they would respond to excess precipitation by increasing photosynthesis. Instead, Virginia NEP variability primarily reflects temperature and PAR anomalies. Colder temperatures, shorter growing seasons, and lack of available radiation tend to limit productivity.

[50] Interannual variability in net ecosystem exchange ( $NEE \sim -NEP$ ) has been quantified through eddy-covariance studies at flux towers. Researchers at Harvard Forest, a hardwood forest in Massachusetts, have assembled a record of net ecosystem exchange since 1991 from eddy-covariance measurements [Goulden *et al.*, 1996; Barford *et al.*, 2001]. Although this ecosystem differs from that of central Virginia, the length of the NEE record has allowed detailed investigation of the forest response to climate variability and long-term management practices. Variability is often expressed as coefficient of variation (CoV), the standard deviation divided by the mean. To a first approximation, the variability derived from the CASA modeling of mid-aged stands is similar to that found at Harvard Forest, both in absolute terms (SD = 29–31 gC for CASA versus 36 for Harvard Forest), as well as in terms of CoV (0.16 for CASA versus 0.18 for Harvard Forest) (Table 1). As noted by Barford *et al.* [2001], interannual variability of NEE at Harvard Forest correlated with climate drivers, including reduced NEE in 1998 due to low temperatures and cloudy conditions.

[51] To date, few forest chronosequences have been monitored with flux towers, and the dependence of flux variability on forest age has not been examined. In this study, we find that forest age influences both the magnitude and sense of NEP response to climate variability (Table 1). The NEP of very young stands is dominated by respiration from soil, roots, litter, and harvest debris. During this stage, warmer temperatures enhance respiration, and increase emissions of CO<sub>2</sub> to the atmosphere. Within a few years, NPP rises dramatically as leaf area increases, and interannual variability of NEP is dominated by NPP effects. During this stage, increased temperatures enhance photosynthesis, and increase uptake of CO<sub>2</sub> from the atmosphere. This pattern continues as the stand ages, although the overall reduction in NPP reduces the NEP variability as well. We suggest, however, that some caution should be exercised regarding expressing variability in terms of CoV. As stands age, average NEP decreases more rapidly than NEP standard deviation, dramatically increasing the CoV value (at equilibrium when NEP = 0 CoV = infinity).

[52] CASA does not explicitly account for autotrophic respiration but rather assumes that it remains a constant fraction of GPP. It is plausible that autotrophic respiration varies independently from GPP and could contribute to

variability in NEP. While the seasonal responses of autotrophic respiration and GPP are likely to be different, a number of studies report that on an annual basis the fraction of GPP that goes to autotrophic respiration is fairly constant (for pine, see Arneeth *et al.* [1998]).

[53] How do disturbance-driven variations in NEP compare to those driven by climate? Houghton [2000] suggested that climate-driven variability should dominate the atmospheric CO<sub>2</sub> anomaly record, since land-cover change is not likely to vary synchronously around the world resulting in cancellation of positive and negative anomalies. On a regional basis, however, variations in land-cover change can have a significant effect. We find that year-to-year variations in rates of land-cover change, harvest, and disturbance could account for 25% of modeled NEP variability. This figure is particular to the ~150 km scale of the study area. It would be expected that, as the area of interest shrinks, the interannual “noise” due to variations in harvest or disturbance rate would be likely to increase. In essence, smaller areas would be more susceptible to random fluctuations in the area cleared. Given that “tall tower” CO<sub>2</sub> concentration measurements typically sample over fetches of ~100 km, it will be important to quantify year-to-year changes in land cover and disturbance in order to interpret these records.

## 6. Conclusions

[54] In this study we explored the integration of biogeochemical modeling, satellite-derived disturbance and photosynthetic measures, and forest inventory data to predict region patterns in NEP and NEP variability. Our key findings include the following. (1) Central Virginia forests acted as a biologic carbon sink during the study year of 1999, with an average biologic NEP of ~80 gC m<sup>-2</sup> yr<sup>-1</sup>, reflecting the balance between high emissions from recent clear-cuts and high uptake by young regrowth. (2) These forests exhibit ~80–130 gC m<sup>-2</sup> yr<sup>-1</sup> of peak-to-peak NEP variability due to climate and fPAR drivers, and about ~30 gC m<sup>-2</sup> yr<sup>-1</sup> due to variability in disturbance rates. (3) NPP and Rh tend to covary in response to climate variations, thus acting as a “buffer” that prevents large swings in NEP. (4) Variability in NEP depends strongly on stand age.

[55] Current initiatives such as the North American Carbon Program require large-area, process-based assessments of carbon fluxes on monthly to annual timescales [Wofsy and Harriss, 2002]. Flux towers are invaluable for understanding the dynamics of specific sites, but their findings cannot easily be extrapolated across large areas [Korner, 2003]. Although regional in scope, this study has relied on biogeochemical modeling to make this extrapolation to scales of ~150 km. Calibrating models to flux and inventory records, and then driving these models with spatially explicit records of vegetation type, climate, and disturbance, constitutes a viable approach for making spatially explicit, continental assessments of carbon fluxes.

[56] However, given the importance of forest age structure for determining both NEP and its variability, the paucity of knowledge on the age structure of the world’s forests (including those of the United States) remains a roadblock for carbon studies. New technologies (such as

spaceborne lidar) as well as improved forest inventories explicitly designed for carbon studies, could improve this situation. Optical data records, such as those from Landsat, can also be useful for characterizing recent forest dynamics across the globe since the 1970s.

[57] **Acknowledgments.** Darrel Williams is thanked for providing the Landsat data used in this study. We also thank two reviewers and the Associate Editor for their constructive comments on the manuscript.

## References

- Adegbidi, H. G., E. J. Jokela, N. B. Comerford, and N. F. Barros (2002), Biomass development for intensively managed loblolly pine plantations growing on spodosols in the southeastern USA, *For. Ecol. Manage.*, *167*, 91–102.
- Albaugh, T. J., H. L. Allen, P. M. Dougherty, and K. H. Johnsen (2004), Long term growth responses of loblolly pine to optimal nutrient and water resource availability, *For. Ecol. Manage.*, *192*, 3–19.
- Arnth, A., F. M. Kelliher, T. M. McSeveny, and J. N. Byers (1998), Net ecosystem productivity, net primary productivity and ecosystem carbon sequestration in a *Pinus radiata* plantation subject to soil water stress, *Tree Physiol.*, *18*, 785–793.
- Barford, C. C., et al. (2001), Factors controlling long- and short-term sequestration of atmospheric CO<sub>2</sub> in a mid-latitude forest, *Science*, *294*, 1688–1691.
- Battle, M., M. L. Bender, P. P. Tans, J. W. C. White, J. T. Ellis, T. Conway, and R. J. Francey (2000), Global carbon sinks and their variability inferred from atmospheric O<sub>2</sub> and δ<sup>13</sup>C, *Science*, *287*, 2467–2470.
- Birdsey, R., and L. Heath (1995), Carbon changes in U.S. forests, in *Productivity of America's Forests and Climate Change*, edited by L. A. Joyce, *Gen. Tech. Rep. RM-GTR-271*, USDA For. Serv., Fort Collins, Colo.
- Bousquet, P., P. Peylin, P. Ciais, C. Le Quere, P. Friedlingstein, and P. P. Tans (2000), Regional changes in carbon dioxide fluxes of land and oceans since 1980, *Science*, *290*, 1342–1346.
- Brown, S. L., and P. E. Schroeder (1999), Spatial patterns of aboveground production and mortality of woody biomass for eastern US forests, *Ecol. Appl.*, *9*, 968–980.
- Caspersen, J. P., S. W. Pacala, J. C. Jenkins, G. C. Hurtt, P. R. Moorcroft, and R. A. Birdsey (2000), Contributions of land-use history to carbon accumulation in US forests, *Science*, *290*, 1148–1151.
- Cohen, W. B., T. A. Spies, R. J. Alig, D. R. Oetter, T. K. Maiersperger, and M. Fiorella (2002), Characterizing 23 years (1972–95) of stand replacement disturbance in western Oregon forests with Landsat imagery, *Ecosystems*, *5*, 122–137.
- Conner, R. C., and A. J. Hartsell (2002), Forest area and conditions, in *Southern Forest Resource Assessment*, edited by D. N. Wear and J. G. Greis, *Gen. Tech. Rep. SRS-53*, 635 pp., USDA For. Serv., Asheville, N. C.
- Curtis, P. S., P. J. Hanson, P. Bolstad, C. Barford, J. C. Randolph, H. P. Schmid, and K. B. Wilson (2002), Biometric and eddy-covariance based estimates of annual carbon storage in five eastern North American deciduous forests, *Agric. For. Meteorol.*, *113*, 3–19.
- Elliott, K. J., L. R. Boring, and W. T. Swank (2002), Aboveground biomass and nutrient accumulation 20 years after clear-cutting a southern Appalachian watershed, *Can. J. For. Res.*, *32*, 667–683.
- Goulden, M. L., J. W. Munger, S. M. Fan, B. C. Daube, and S. C. Wofsy (1996), Exchange of carbon dioxide by a deciduous forest: Response to interannual climate variability, *Science*, *271*, 1576–1578.
- Gower, S. T., J. Vogel, J. M. Norman, C. J. Kucharik, S. J. Steele, and T. K. Stow (1997), Carbon distribution and aboveground net primary production in aspen, jack pine and black spruce stands in Saskatchewan and Manitoba, Canada, *J. Geophys. Res.*, *102*(D24), 29,029–29,041.
- Hamilton, J. G., E. H. DeLucia, K. George, S. L. Naidu, A. C. Finzi, and W. H. Schlesinger (2002), Forest carbon balance under elevated CO<sub>2</sub>, *Oecologia*, *131*, 250–260.
- Hansen, J., R. Ruedy, J. Glasco, and M. Sato (1999), GISS analysis of surface temperature change, *J. Geophys. Res.*, *104*(D24), 30,997–31,022.
- Hicke, J. A., G. P. Asner, J. T. Randerson, C. Tucker, S. Los, R. Birdsey, J. C. Jenkins, and C. Field (2002), Trends in North American net primary productivity derived from satellite observations, 1982–1998, *Global Biogeochem. Cycles*, *16*(2), 1018, doi:10.1029/2001GB001550.
- Hicke, J. A., G. P. Asner, E. S. Kasischke, N. H. French, J. T. Randerson, G. J. Collatz, B. J. Stocks, C. J. Tucker, S. O. Los, and C. B. Field (2003), Postfire response of North American boreal forest net primary productivity analyzed with satellite observations, *Global Change Biol.*, *9*, 1145–1157.
- Houghton, R. A. (2000), Interannual variability in the global carbon cycle, *J. Geophys. Res.*, *105*(D15), 20,121–20,130.
- Houghton, R. A., J. L. Hackler, and K. T. Lawrence (1999), The U.S. carbon budget: Contributions from land-use change, *Science*, *285*, 574–578.
- Huffman, G. J., R. F. Adler, P. Arkin, A. Chang, R. Ferraro, A. Gruber, J. Janowiak, A. McNab, B. Rudolf, and U. Schneider (1997), The Global Precipitation Climatology Project (GPCP) Combined Precipitation Dataset, *Bull. Am. Meteorol. Soc.*, *78*(1), 5–20.
- Hurtt, G. C., S. W. Pacala, P. R. Moorcroft, J. Caspersen, E. Shevliakova, R. A. Houghton, and B. Moore (2002), Projecting the future of the US carbon sink, *Proc. Natl. Acad. Sci.*, *99*, 1389–1394.
- Janssens, I. A., et al. (2001), Productivity overshadows temperature in determining soil and ecosystem respiration across European forests, *Global Change Biol.*, *7*, 269–278.
- Jenkins, J. C., R. A. Birdsey, and Y. Pan (2001), Biomass and NPP estimation for the mid-Atlantic region (USA) using plot-level forest inventory data, *Ecol. Appl.*, *11*, 1174–1193.
- Johnson, D. W., and P. S. Curtis (2001), Effects of forest management on soil C and N storage: Meta analysis, *For. Ecol. Manage.*, *140*, 227–238.
- Jokela, E. J., and T. A. Martin (2000), Effects of ontogeny and soil nutrient supply on production, allocation, and leaf area efficiency in loblolly and slash pine stands, *Can. J. For. Res.*, *30*, 1511–1524.
- Jokela, E. J., P. M. Dougherty, and T. A. Martin (2004), Production dynamics of intensively managed loblolly pine stands in the southern United States: A synthesis of seven long-term experiments, *For. Ecol. Manage.*, *192*, 117–130.
- Knapp, A. K., and M. D. Smith (2001), Variation among biomes in temporal dynamics of aboveground primary production, *Science*, *291*, 481–484.
- Knoepp, J. D., and W. T. Swank (1997), Forest management effects on surface soil carbon and nitrogen, *Soil Sci. Soc. Am. J.*, *61*, 928–935.
- Korner, C. (2003), Slow in, rapid out—Carbon flux studies and Kyoto targets, *Science*, *300*, 1242–1243.
- Law, B. E., O. J. Sun, J. Campbell, S. Van Tuyl, and P. E. Thornton (2002), Changes in carbon storage and fluxes in a chronosequence of ponderosa pine, *Global Change Biol.*, *9*, 510–524.
- Le Houerou, H. N., L. Bingham, and W. Skerbek (1988), Relationship between the variability of primary production and variability of annual precipitation in world arid lands, *J. Arid Environ.*, *15*, 1–18.
- Litvak, M., S. Mille, S. C. Wofsy, and M. Goulden (2003), Effect of stand age on whole ecosystem CO<sub>2</sub> exchange in the Canadian boreal forest, *J. Geophys. Res.*, *108*(D3), 8225, doi:10.1029/2001JD000854.
- Los, S. O., G. J. Collatz, P. J. Sellers, C. M. Malmstrom, N. H. Pollack, R. S. DeFries, L. Bounoua, M. T. Parris, C. J. Tucker, and D. A. Dazlich (2000), A global 9-yr biophysical land surface dataset from NOAA AVHRR data, *J. Hydrometeorol.*, *1*, 183–199.
- McGuire, A. D., et al. (2001), Carbon balance of the terrestrial biosphere in the twentieth century: Analysis of CO<sub>2</sub> climate and land use effects with four process-based ecosystem models, *Global Biogeochem. Cycles*, *15*, 183–206.
- Nemani, R., M. White, P. Thornton, K. Nishida, S. Reddy, J. Jenkins, and S. Running (2002), Recent trends in hydrologic balance have enhanced the terrestrial carbon sink in the United States, *Geophys. Res. Lett.*, *29*(10), 1468, doi:10.1029/2002GL014867.
- Odum, E. P. (1969), The strategy of ecosystem development, *Science*, *164*, 262–270.
- Pacala, S. W., et al. (2001), Consistent land- and atmosphere-based US carbon sink estimates, *Science*, *292*, 2316–2320.
- Potter, C. S., J. T. Randerson, C. B. Field, P. A. Matson, P. M. Vitousek, H. A. Mooney, and S. A. Klooster (1993), Terrestrial ecosystem production: A process model-based on global satellite and surface data, *Global Biogeochem. Cycles*, *7*, 811–841.
- Pregitzer, K. S., and E. Euskirchen (2004), Carbon cycling and storage in world forests: Biome patterns related to forest age, *Global Change Biol.*, *10*, 2052–2077.
- Prisley, S. P., and A. J. Malmquist (2002), Impacts of rotation age changes on growth/removals ratios, *South. J. Appl. For.*, *26*, 72–77.
- Randerson, J. T., F. S. Chapin, J. W. Harden, J. C. Neff, and M. E. Harmon (2002), Net ecosystem production: A comprehensive measure of net carbon accumulation by ecosystems, *Ecol. Appl.*, *12*, 937–947.
- Richard, Y., and I. Poccard (1998), A statistical study of NDVI sensitivity to seasonal and interannual rainfall variation in Southern Africa, *Int. J. Remote Sens.*, *19*, 2907–2929.
- Richer, D. D., D. Markewitz, S. E. Trumbore, and C. G. Wells (1999), Rapid accumulation and turnover of soil carbon in a re-establishing forest, *Nature*, *400*, 56–58.
- Saleska, S. R., et al. (2003), Carbon in Amazon forests: Unexpected seasonal fluxes and disturbance-induced losses, *Science*, *302*, 1554–1557.

- Samuelson, L. J., K. Johnsen, and T. Stokes (2004), Production, allocation, and stemwood growth efficiency of *Pinus taeda* L. stands in response to 6 years of intensive management, *For. Ecol. Manage.*, *192*, 59–70.
- Siry, J. P. (2002), Intensive timber management practices, in Southern Forest Resource Assessment, edited by D. N. Wear and J. G. Greis, *Gen. Tech. Rep. SRS-53*, 635 pp., South. Res. Stn., USDA For. Serv., Asheville, N. C.
- Smith, J. E., L. S. Heath, and J. C. Jenkins (2003), Forest volume-to-biomass models and estimates of mass for live and standing dead trees of U.S. Forests, general technical report, Northeast. Res. Stn., USDA For. Serv., Newtown Square, Pa.
- Swank, W. T., J. M. Vose, and K. J. Elliot (2001), Long-term hydrologic and water quality responses following commercial clearcutting of mixed hardwoods on a southern Appalachian catchment, *For. Ecol. Manage.*, *143*, 163–178.
- Thornton, P. E., et al. (2002), Modeling and measuring the effects of disturbance history and climate on carbon and water budgets in evergreen needleleaf forests, *Agric. For. Meteorol.*, *113*, 185–222.
- Tucker, C. J., J. E. Pinzon, M. E. Brown, D. Slayback, E. W. Pak, R. Mahoney, E. Vermote, and N. El Saleous (2006), An extended AVHRR 8-km NDVI data set compatible with MODIS and SPOT vegetation NDVI data, *Int. J. Remote Sens.*, in press.
- Turner, D. P., G. J. Koerper, M. E. Harmon, and J. J. Lee (1995), A carbon budget for forests of the conterminous United States, *Ecol. Appl.*, *5*, 421–436.
- van der Werf, G. R., J. T. Randerson, G. J. Collatz, L. Giglio, P. S. Kasibhatla, A. F. Arellano, S. C. Olsen, and E. S. Kasischke (2004), Continental-scale partitioning of fire emissions during the 1997 to 2001 El Niño/La Niña period, *Science*, *303*, 73–76.
- Wofsy, S. C., and R. C. Harriss (2002), The North American Carbon Program (NACP): Report of the NACP Committee of the U.S. Inter-agency Carbon Cycle Science Program, report, U.S. Global Change Res. Program, Washington, D. C.
- Zhang, Y.-C., W. B. Rossow, A. A. Lacis, V. Oinas, and M. I. Mishchenko (2004), Calculation of radiative fluxes from the surface to top of atmosphere based on ISCCP and other global data sets: Refinements of the radiative transfer model and the input data, *J. Geophys. Res.*, *109*, D19105, doi:10.1029/2003JD004457.

---

G. J. Collatz and J. G. Masek, Biospheric Sciences Branch, NASA Goddard Space Flight Center, Greenbelt, MD 20771, USA. (jeffrey.g.masek@nasa.gov)